Available online www.jocpr.com

Journal of Chemical and Pharmaceutical Research, 2015, 7(7):105-116

Research Article

ISSN : 0975-7384
CODEN(USA) : JCPRC5

Electrochemical studies of the corrosion inhibition property of *Rosmarinus officinalis* on mild steel in dilute sulphuric acid

R. T. Loto[1,2]*, R. O. Loto[3], O. O. Joseph[1] and I. Akinwumi[4]

[1]Department of Mechanical Engineering, Covenant University, Ota, Ogun State, Nigeria
[2]Department of Chemical, Metallurgical & Materials Engineering, Tshwane University of Technology, Pretoria, South Africa
[3]Department of Metallurgical and Materials Engineering, University of Lagos, Akoka, Lagos, Nigeria
[4]Department of Civil Engineering, Covenant University, Ota, Ogun State, Nigeria

---

ABSTRACT

The electrochemical behaviour and corrosion inhibition of mild steel in 0.5M and 1M dilute sulpuric acid by rosemary oil (Rosmarinus officinalis) at ambient temperature was investigated through potentiodynamic polarization test, weight loss techniques analysis and optical microscopy. Results obtained showed the organic compound to be highly effective with a maximum inhibition efficiency of 80.8 % and 87.9% from weight loss and 84.1% and 80.8% from polarization test in the acid test solutions. The adsorption characteristics of the compound obeyed the Langmuir adsorption isotherm while the inhibition mechanism was observed from thermodynamic calculations to be physiochemical. Optical microscopy micrographs confirms the overwhelming influence of the compound on the topography and surface morphology of the steel after exposure.

Keywords: carbon steel; corrosion resistance; anodic protection; adsorption; organic inhibitor

---

INTRODUCTION

Mild steel is widely applied in a range of technological applications, however its poor corrosion resistance and susceptibility in acidic conditions limits its versatility [1-3]. Acid solutions are generally used in industrial operations such as pickling, cleaning, descaling, oil well acidizing etc. [4, 5]. Corrosion in the petroleum industry arises at all operational levels from down-hole through surface equipment and devices to processing facilities. It can be observed in the form of leakage in tanks, casings, tubing, pipelines, and in other equipment [6-8]. Corrosion problems are usually compounded and sometimes complicated due to the connection between operating problems and facility maintenance leading limited or complete cessation of the flow process [9]. Among other corrosion control processes the application of corrosion inhibitors has been proven to be versatile and effective [10, 11]. Corrosion inhibitors are widely applied to weaken the corrosive effect of aggressive environments on metallic alloys [12]. Selection and application of inhibitor is subject to its cost, toxicity, availability and efficiency to inhibit corrosion and alleviate the environmental impact on the substrate alloy. Previous research has shown that most of the high performance inhibitors are organic compound containing nitrogen, oxygen and/or sulphur atoms [13-23]. The electrochemical behavior of these compounds is credited to its adsorption onto the metal/solution interface. This investigation aims to study the electrochemical behaviour, corrosion inhibition characteristics and adsorption mechanism of rosemary oil (ROS) on mild steel in 0.5 M and 1 M H_2SO_4 solution.

EXPERIMENTAL SECTION

Material specimen

Mild steel obtained commercially and analyzed at the Advanced Materials and Tribo-Corrosion Research Laboratory, Department of Chemical and Metallurgical Engineering, Tshwane University of Technology, South Africa gave a percentage weight composition of 0.401% C, 0.169% Si, 0.440% Mn, 0.005% P, 0.012% S, 0.080% Cu, 0.008% Ni, and 0.025% Al, with the rest composed of Fe. The specimen dimension is cylindrical with 14 mm diameter.

Inhibiting compound

Rosemary oil (rosmarinus officinalis), an oily yellow transparent liquid is the organic compound used as the corrosion inhibitor. It has a boiling point of 176 °C, the density is 0.908 g/mL at 25 °C, a refractive index of n20/D 1.468 and flash point of 121 °

Test Solution

0.5M & 1M H_2SO_4, prepared from of Analar grade H_2SO_4 were used as the corrosion test solution.

Preparation of the steel specimens

The mild steels (14 mm diameter) were mechanically cut into specific dimensions of 10 m average lenght. The exposed ends of each steel were metallographically prepared with silicon carbide abrasive papers of 80, 120, 220, 800 and 1000 grits, washed with distilled water, rinsed with acetone, dried and stored in a dessicator for weight loss test analysis and potentiodynamic polarization.

Weight-loss Experiments

The steel samples were each immersed in 200ml of the acid solution at predetermined volumetric concentrations of rosemary oil (ROS) for 360h at 25^{o}C ambient temperature. Each sample was analysed every 72h i.e. washed with distilled water, rinsed with acetone, dried and weighed. Graphical plots of inhibition efficiency (%*IE*) versus exposure time (h) (Figs. 1 & 2) for the test media were made from the obtained data Tables 1 & 2.

The corrosion rate (*C*) wass determined from Equation 1:

$$R = \left[\frac{87.6M}{DAT}\right] \quad (1)$$

M is the weight loss (mg), *D* is the density (g/cm^2), *A* is the surface area in cm^2, and *T* is the exposure time (h). The %*IE* was calculated from Equation 2 below.

$$\%IE = \left[\frac{C_1 - C_2}{C_1}\right] \times 100 \quad (2)$$

Where C_1 and C_2 are the corrosion rates with and without of predetermined concentration of TPD. The surface coverage is calculated from Equation 3:

$$\theta = \left[1 - \frac{M2}{M1}\right] \quad (3)$$

Where θ is the quantity of TPD adsorbed per gram (or kg) of the steel surface. M_1 and M_2 are the weight loss of carbon steel specimen in the free and inhibited test media.

Potentiodynamic Polarization

Potentiodynamic polarization tests were performed with the aid of cylindrical steel samples embedded in resin mounts with exposed surface of 154 mm^2. The working electrodes were polished with differential grades of silicon carbide paper, rinsed with distilled water and dried with acetone. Polarization tests were performed at ambient temperature of 25 ^{o}C with Digi-Ivy potentiostat. A platinum rod was used as the counter electrode and silver chloride electrode (Ag/AgCl) with pH of 6.5 was used as the reference electrode. The potentials were scanned from -1.5V to +1.5 V at a scan rate of 0.002V/s. The corrosion current (i_{corr}), corrosion current density (I_{corr}) and

corrosion potential (E_{corr}) were determined from the Tafel plots of potential versus log I_{corr}. The corrosion rate (R), the degree of surface coverage (θ) and the percentage inhibition efficiency (%IE) were calculated from Equation 4;

$$R = \frac{0.00327 \times I\text{corr} \times E\text{q}}{D} \quad (4)$$

Where I_{corr} is the current density (μA/cm^2), D is the density (g/cm^3), Eq is the specimen equivalent weight (g);

The percentage inhibition efficiency (%IE) was calculated from corrosion the corrosion rate as shown in Equation 5;

$$\%IE = 1 - \left[\frac{C_2}{C_1}\right] \times 100 \quad (5)$$

$C_1$and C_2 are the corrosion rates in absence and presence of TPD respectively.

Optical Microscopy Characterization

The surface morphology of the inhibited and non-inhibited steel samples were further studied after weight-loss analysis with the aid of Zenith metallurgical microscope for which micrographs were taken.

RESULTS AND DISCUSSION

Weight-loss measurements

Increase in ROS concentration results in a progressive decrease in corrosion rate and increase in inhibition efficiency as shown in Tables 1 & 2. The inhibitor molecules attached themselves onto the alloy surface through adsorption in the acid solution inhibiting the electrolytic transport of the anionic corrosive species responsible for the deterioration of the steel. Organic inhibitors generally have heteroatoms. O, N, and S are found to have higher basicity and electron density and thus act as corrosion inhibitor. O, N, and S are the active centers for the process of adsorption on the metal surface [24]. The marked difference between the inhibited and uninhibited samples is due to the presence of ROS and its electrochemical influence on the oxygen reduction, hydrogen evolution and oxidation corrosion process, invariably protecting the steel surface. Table 2 shows greater aggression of the acid medium as compared to Table 1 for the uninhibited sample (sample A) due to increased concentration of the acid from 0.5M to 1M. Fig. 1(a & b) shows the corrosion rate and inhibition efficiency versus exposure time for mild steel in 0.5 M H_2SO_4, while Fig. 2(a & b) shows the corrosion rate and inhibition efficiency versus exposure time for mild steel in 1 M H_2SO_4. The graph depicts the overwhelming influence of ROS after addition in the acid solutions.

Table 1: Data obtained from weight loss measurements for mild steel in 0.5 M H_2SO_4 at specific concentrations of the ROS after 360 h

Sample	Weight Loss (g)	Corrosion Rate (mm/y)	Inhibitor Conc. (M)	Inhibitor Conc. (%)	Inhibition Efficiency (%)	Surface Coverage (θ)
A	1.889	7.46	0	0	0	0
B	0.359	0.85	1.25E-05	1.25	81.0	0.8099
C	0.446	1.66	2.50E-05	2.50	76.4	0.7637
D	0.297	1.50	3.75E-05	3.75	84.3	0.8428
E	0.225	0.95	5.00E-05	5.00	88.1	0.8811
F	0.325	1.28	6.25E-05	6.25	82.8	0.8280
G	0.362	1.33	7.50E-05	7.50	80.8	0.8081

Table 2: Data obtained from weight loss measurements for mild steel in 1 M H_2SO_4 at specific concentrations of the ROS after 360 h

Sample	Weight Loss (g)	Corrosion Rate (mm/y)	Inhibitor Conc. (M)	Inhibitor Conc. (%)	Inhibition Efficiency (%)	Surface Coverage (θ)
A	3.179	15.53	0	0	0	0
B	0.765	3.32	1.25E-05	1.25	75.9	0.7595
C	0.402	1.63	2.50E-05	2.50	87.4	0.8736
D	0.340	1.25	3.75E-05	3.75	89.3	0.8930
E	0.168	0.70	5.00E-05	5.00	94.7	0.9471
F	0.359	1.24	6.25E-05	6.25	88.7	0.8872
G	0.384	1.56	7.50E-05	7.50	87.9	0.8792

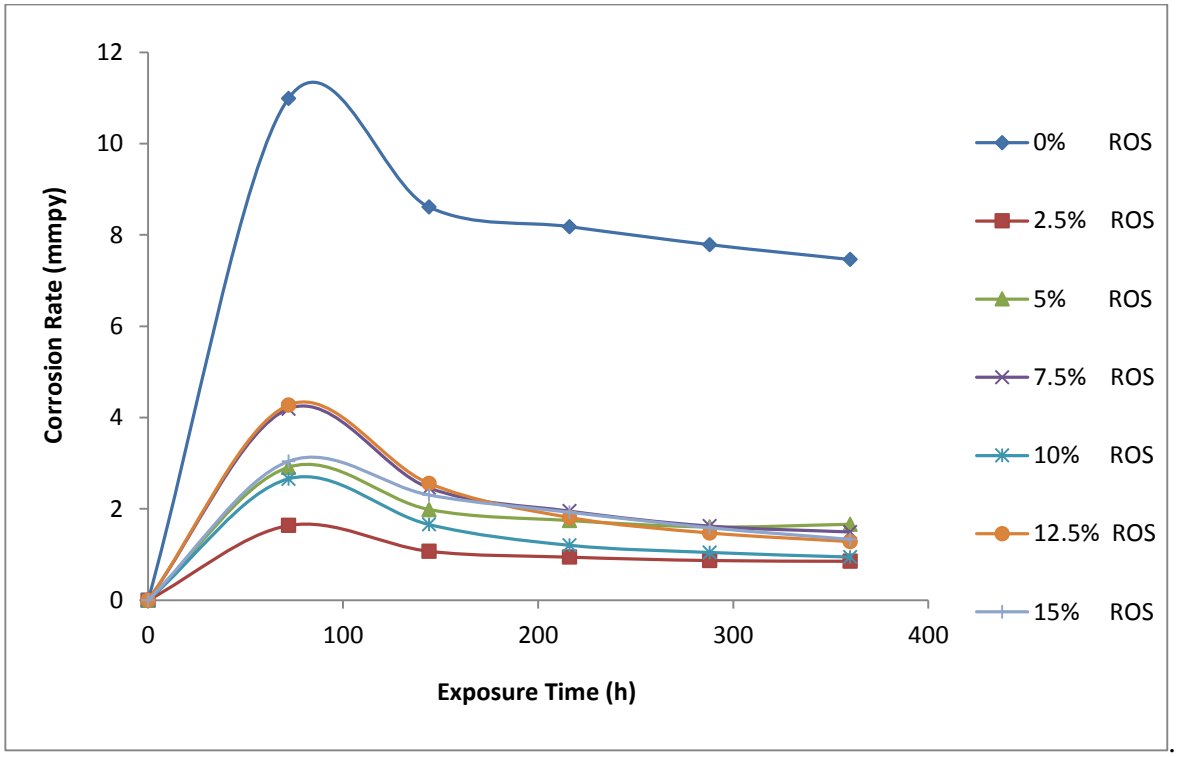

(a)

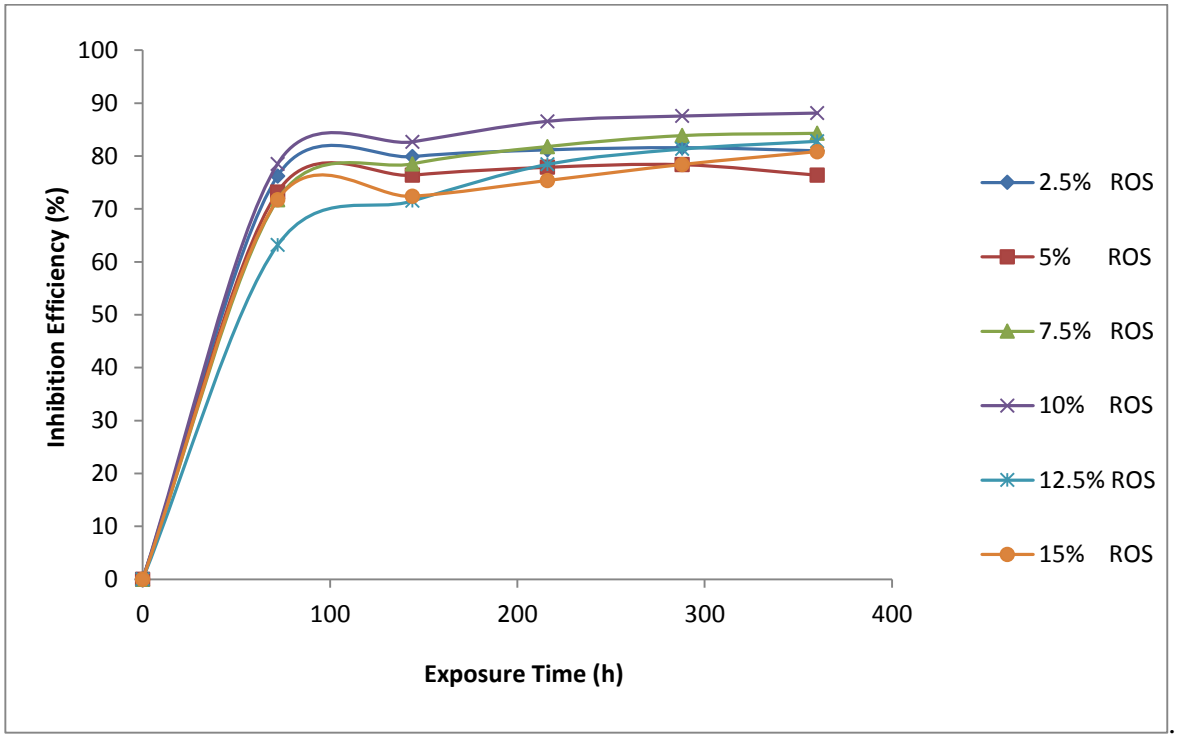

(b)

Figure 1: Graph of (a) corrosion rate versus exposure time (b) inhibition efficiency versus exposure time in 0.5 M H_2SO_4 at 0%-15% ROS

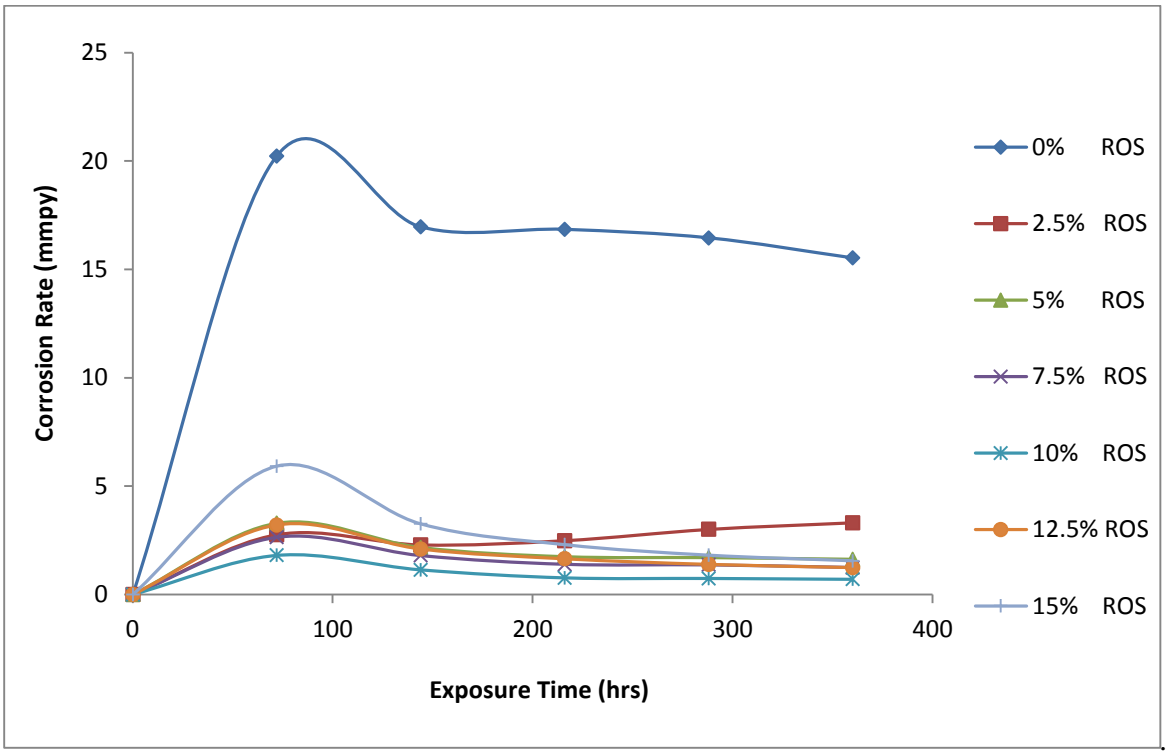

(a)

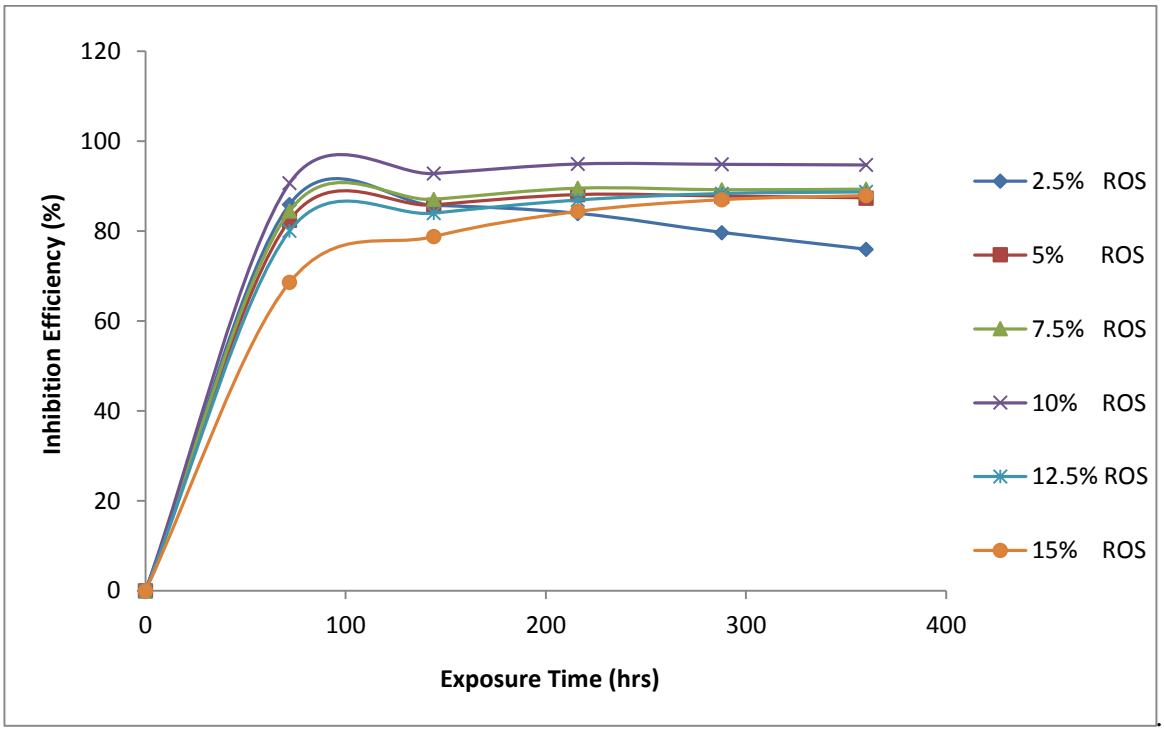

(b)

Figure 2: Graph of (a) corrosion rate versus exposure time (b) inhibition efficiency versus exposure time in 1 M H_2SO_4 at 0%-15% ROS

Potentiodynamic polarization resistance

ROS adsorption onto the steel surface is independent of the value of its concentrations in both solutions as shown in Table 3 & 4 respectively; from the lowest to the highest concentration of ROS the inhibition efficiency is generally the same. Data from the tables show that the adsorbed inhibiting compound retarded the electrochemical process of corrosion with significant influence on the electrochemical parameters after 0% ROS. In Fig. (3 & 4) the corrosion potential shifts towards more positive potentials with increase in ROS concentrations. This indicates anodic inhibition through film formation which stifles the redox electrochemical process responsible for corrosion at the steel solution interface. The film also acts as barrier against the corrosive species in the acid solution. Fig. 3 shows the polarization plots exhibits similar electrochemical behavior over the potential domain but in Fig. 4 there are significant variations in corrosion potential. The variations are explained on the basis of competitive adsorption between the inhibitor molecules trying to stifle the redox corrosion process through blockage of the reactive sites by physisorption and chemical interaction through electron sharing, and the corrosive specie [25, 26]. This invariably affects the redox reaction process under potential difference resulting changes in potential. The corrosion current is the product of the electron flow as a result of the redox reaction process and thermodynamics of the corroding system. The maximum displacement in E_{corr} values is -13 mV in 0.5 M H_2SO_4 and 83mV in 1 M H_2SO_4 thus it is a mixed type inhibitor with greater tendency for anodic inhibition in the acid solution [27].

Table 3 Data obtained from polarization resistance measurements for mild steel in 0.5 M H_2SO_4 at specific concentrations of the ROS

Corrosion Potential (E_{corr}) (v)	Corrosion Current (I_{corr}) (A)	Current density (I_{corr}) (A/cm^2)	bc (v)	ba (v)	Polarization Resistance (R_p)(Ω)	Corrosion Rate (mm/year)	Inhibition Efficiency (%)
-0.383	9.22E-04	5.98E-04	-0.766	0.071	37.15	6.95	0
-0.387	2.06E-04	1.34E-04	-0.910	0.191	511.26	1.55	77.68
-0.396	1.62E-04	1.05E-04	-0.885	0.185	628.10	1.22	82.42
-0.387	1.77E-04	1.15E-04	-0.702	0.174	569.12	1.33	80.82
-0.393	1.54E-04	1.00E-04	-0.874	0.202	741.20	1.16	83.27
-0.394	1.73E-04	1.13E-04	-0.798	0.170	541.59	1.31	81.17
-0.398	1.41E-04	9.12E-05	-0.884	0.185	724.12	1.06	84.75

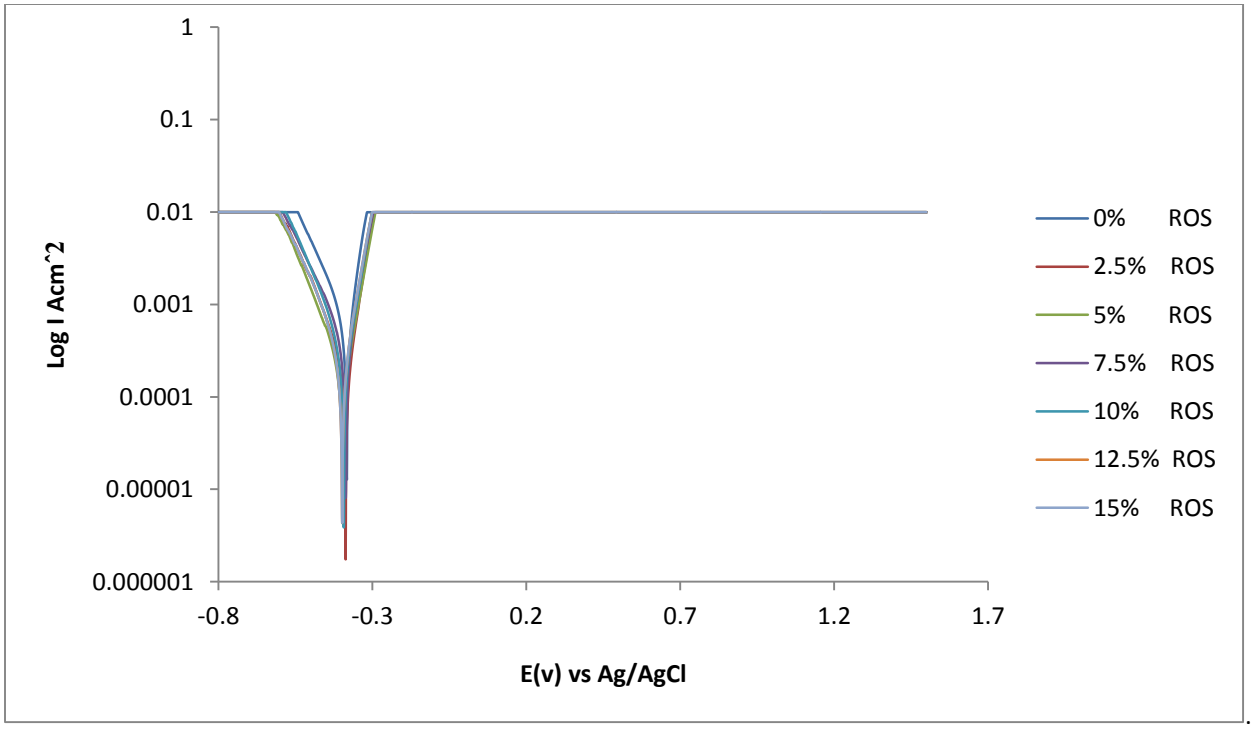

Figure 3: Comparison plot of cathodic and anodic polarization scans for mild steel in 0.5 M H_2SO_4 solution at (0% - 15%) ROS

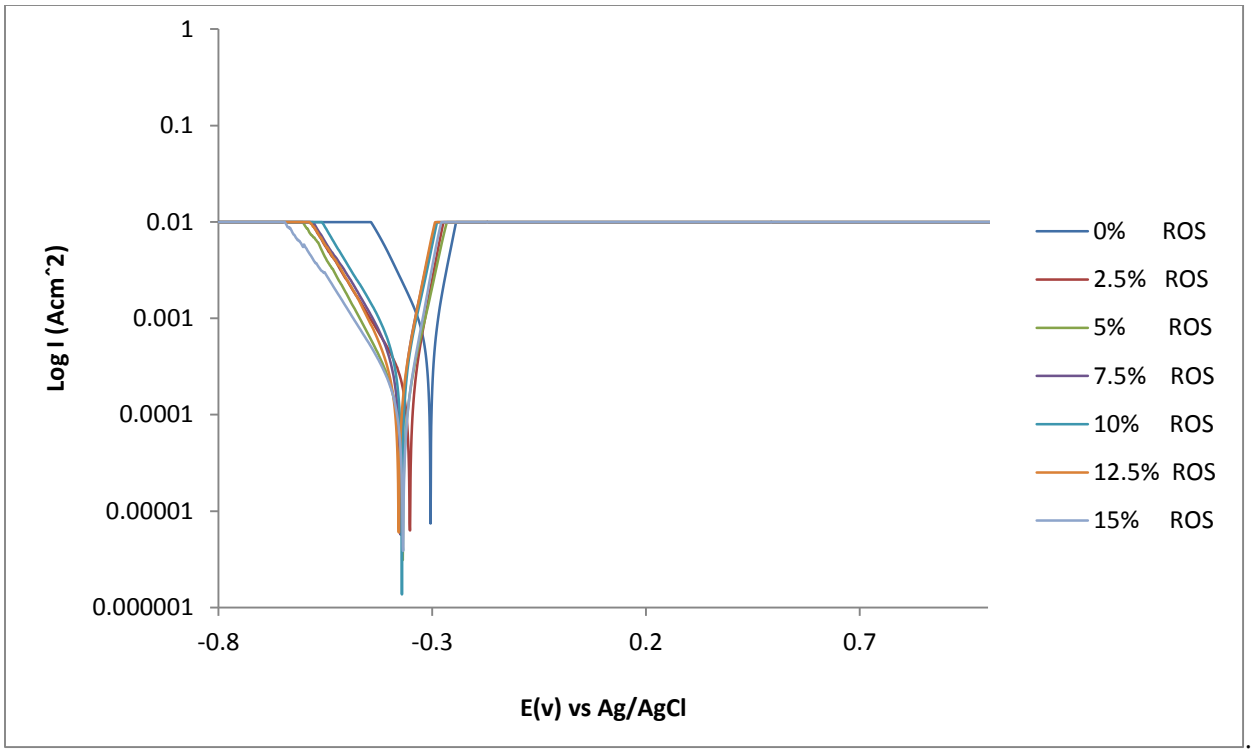

Figure 4: Comparison plot of cathodic and anodic polarization scans for mild steel in 1 M H_2SO_4 solution at (0% - 15%) ROS

Table 4 Data obtained from polarization resistance measurements for mild steel in 1 M H_2SO_4 at specific concentrations of the ROS

Corrosion Potential (E_{corr}) (v)	Corrosion Current (I_{corr}) (A)	Current density (I_{corr}) (A/cm^2)	bc (v)	ba (v)	Polarization Resistance (R_p)(Ω)	Corrosion Rate (mm/year)	Inhibition Efficiency (%)
-0.304	1.13E-03	7.31E-04	-0.923	0.043	17.41	8.50	0
-0.352	1.76E-04	1.14E-04	-0.747	0.139	422.63	1.33	80.93
-0.369	2.02E-04	1.31E-04	-0.860	0.204	577.04	1.52	78.12
-0.374	1.46E-04	9.49E-05	-0.791	0.164	615.75	1.10	84.14
-0.371	1.24E-04	8.07E-05	-0.788	0.172	769.54	0.94	86.51
-0.387	2.11E-04	1.37E-04	-0.888	0.186	485.97	1.59	77.15
-0.368	2.16E-04	1.40E-04	-0.749	0.223	638.32	1.63	76.52

Adsorption Isotherm

Adsorption isotherm was applied to explain the inhibition mechanism of ROS on the steel surface determination of the mechanism of metal/inhibitor interactions due to the formation of complexes between the inhibitor molecules and the valence atoms metal [27]. Langmuir adsorption isotherm produced the best fit in the acid solutions. The deviation of the slopes from unity in Fig. 11 is the result of molecular interaction among the adsorbed inhibitor anions and changes in the values of Gibbs free energy of adsorption with increase in surface coverage. The fitted line gave a value less than unity for the slopes. This suggests a slight deviation from ideal conditions assumed in Langmuir model.

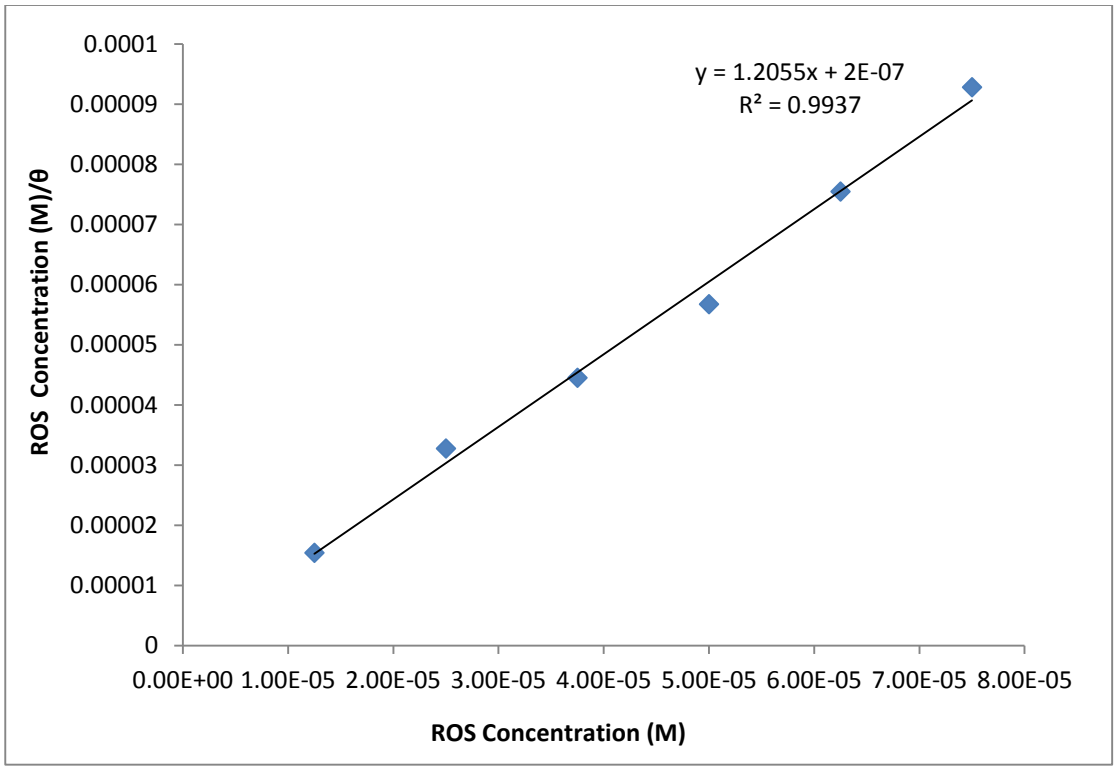

(a)

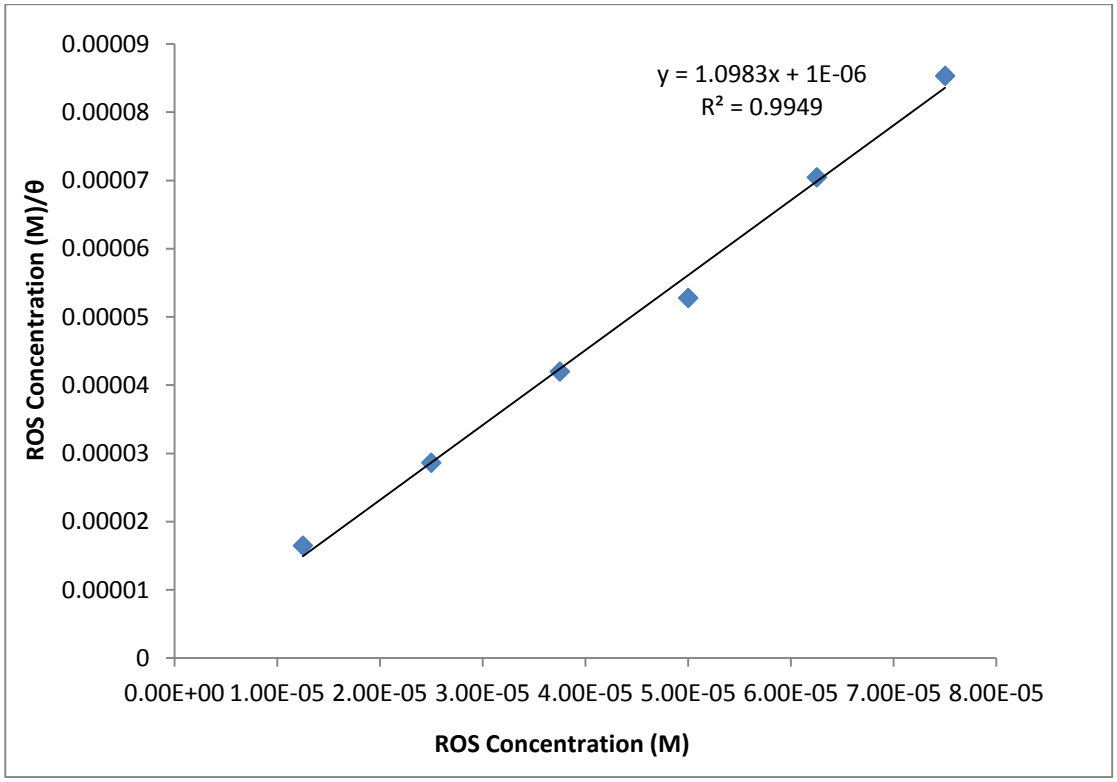

(b)

Figure 4: Relationship between $\frac{C}{\theta}$ and inhibitor concentration (M) in (a) 0.5 M H_2SO_4 (b) 1 M H_2SO_4

Thermodynamics of the corrosion process

Table 5 shows the values of Gibbs free energy, surface coverage and equilibrium constant of adsorption of the corrosion inhibition mechanism. The negative values of ΔG_{ads} showed the spontaneous nature of the adsorption process [28]. The calculated values of ΔG_{ads} ranges between −27.10 and −35.55 kJ mol^{-1} for ROS in 0.5 M H_2SO_4 while the value in 1 M H_2SO_4 ranged between −31.67 and −28.47 kJ mol−1. The inhibition mechanism is generally physiochemical in both solutions.

Table 5 Data obtained for the values of Gibbs free energy, surface coverage and equilibrium constant of adsorption at specific concentrations of ROS in 0.5 M H_2SO_4

Sample	Surface Coverage (θ)	Equilibrium constant of adsorption (K)	Gibbs free energy (ΔG_{ads})
A	0	0	0
B	0.8099	340735.0	-31.55
C	0.7637	129312.1	-29.16
D	0.8428	142949.5	-29.44
E	0.8811	148144.2	-29.50
F	0.8280	77001.8	-27.90
G	0.8081	56150.8	-27.10

Table 5 Data obtained for the values of Gibbs free energy, surface coverage and equilibrium constant of adsorption at specific concentrations of ROS in 1 M H_2SO_4

Sample	Surface Coverage (θ)	Equilibrium constant of adsorption (K)	Gibbs free energy (ΔG_{ads})
A	0	0	0
B	0.7595	252607.9	-30.81
C	0.8736	276544.7	-31.04
D	0.8930	222658.8	-30.53
E	0.9471	357990.5	-31.67
F	0.8872	125836.0	-29.10
G	0.8792	97073.9	-28.47

.

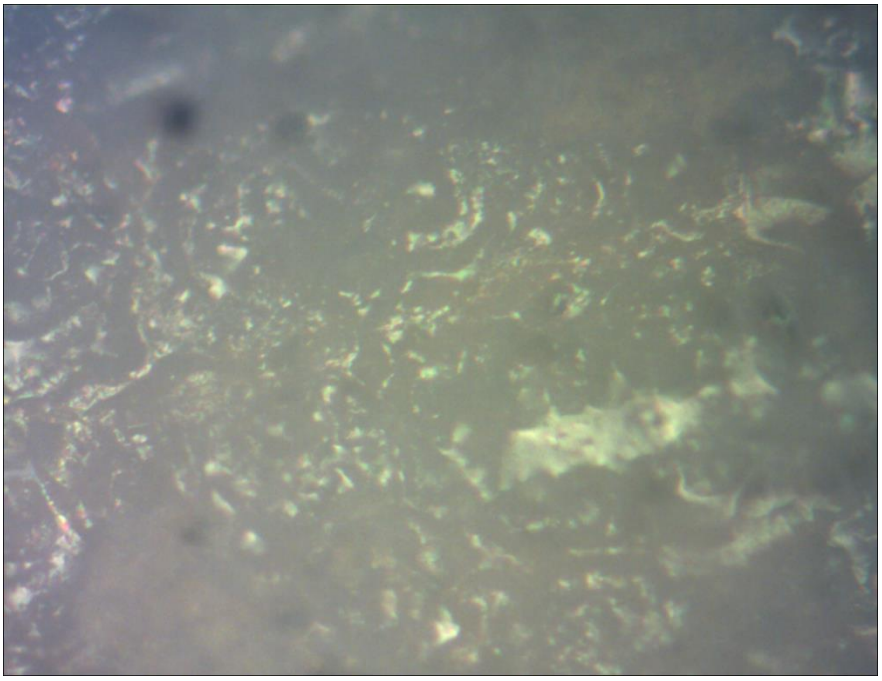

(a)

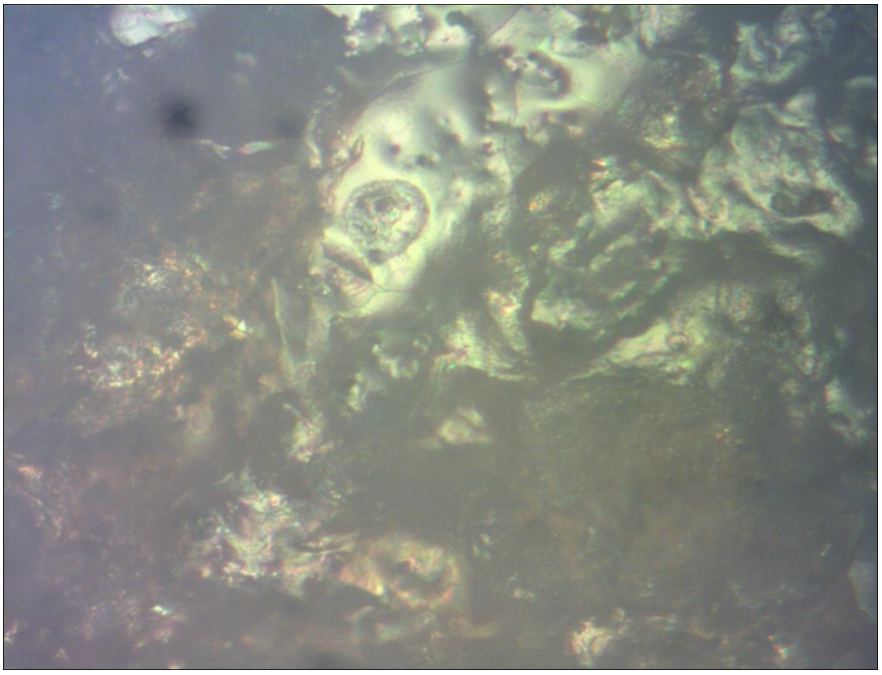

(b)

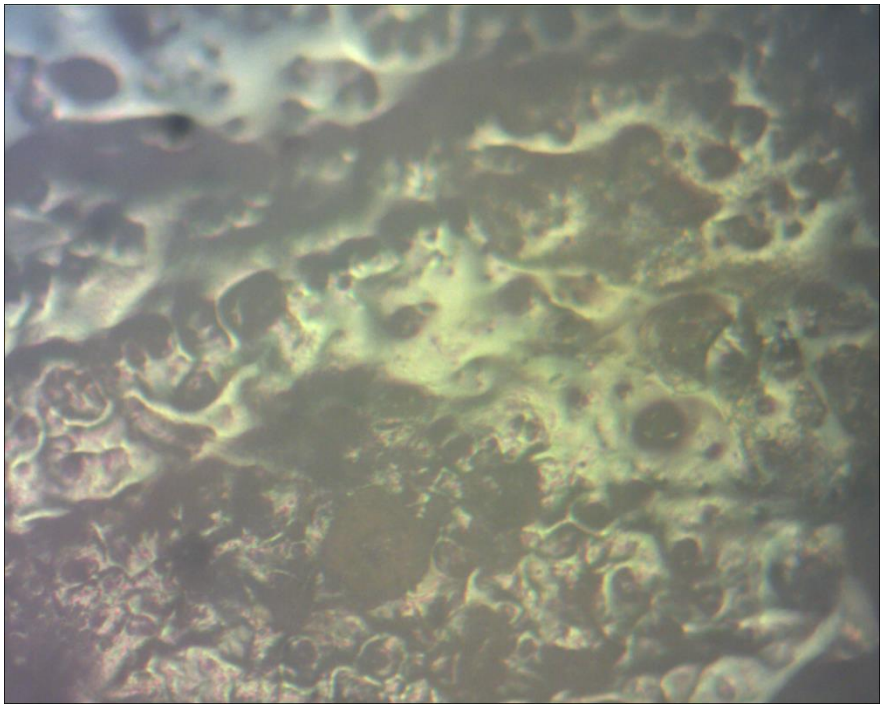

(c)

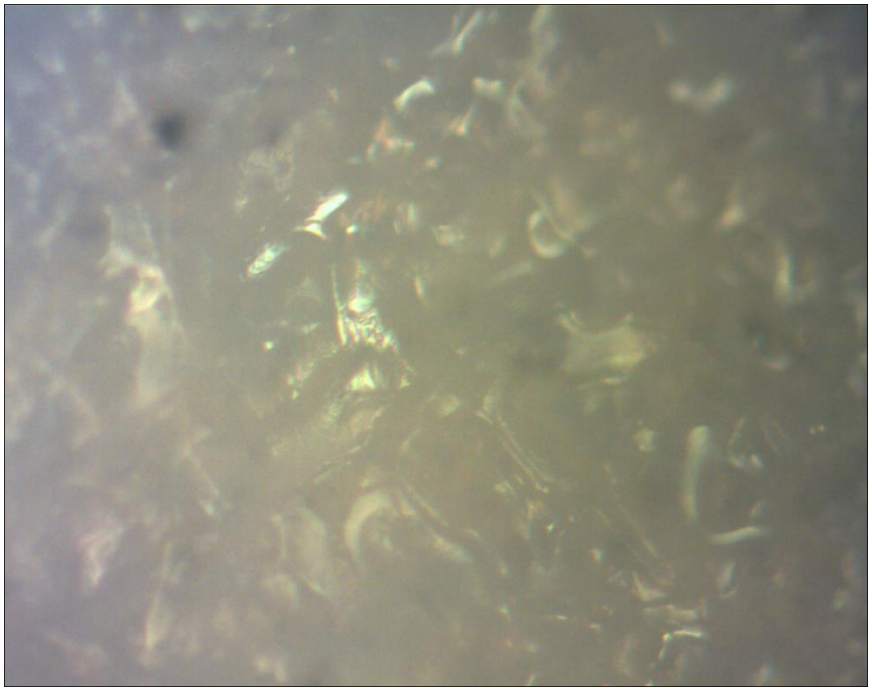

(d)

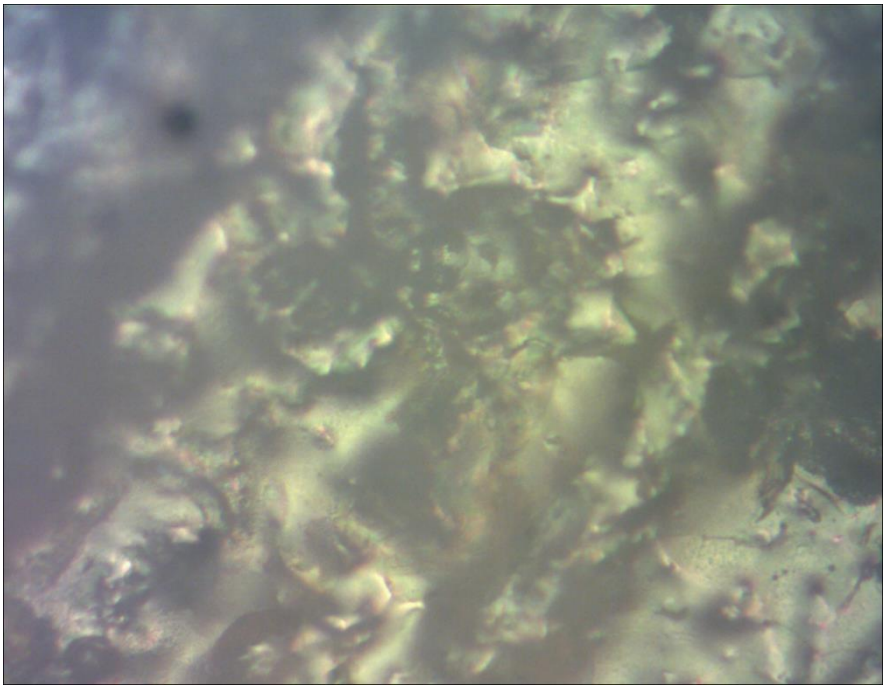

(e)

Figure 5: Optical micrographs at mag. x50 of: a) mild steel before immersion, b) mild steel after immersion in 0.5 M H_2SO_4, c) mild steel after immersion in 1 M H_2SO_4, d) mild steel after immersion in 0.5 M H_2SO_4 with ROS compound, e) mild steel after immersion in 1 M H_2SO_4 with ROS compound

Optical Microscopy

The micrographs in Fig. 5 shows the variation in surface topography of the steel before and after immersion in the acid solution with and without ROS compound in the acid solution. Fig. 5a shows the steel surface before immersion

in the acid solution while Fig. 5(b & c) shows the surface topography after immersion in the acid solution without ROS compound. The remarkable changes is due to the debilitating effect of the corrosive ions involving the electrochemical action of the sulphate species of the acid on the steel which results in deterioration of its surface properties. The degree of deterioration is much more significant in Fig.5c compared to Fig. 5b. The surface topography in Fig. 5(d & e) is due to the precipitation and surface coverage of an invisible film of ROS molecules in the acid solution onto the steel surface throughout the exposure period through diffusion and adsorption. This invariable protects the surface properties of the steel after immersion in the acid solutions.

CONCLUSION

Rosemary oil showed excellent corrosion inhibition; reducing the corrosion rate of mild steel at all concentrations studied from weight-loss and potentiodynamic polarization tests. The inhibition efficiency was observed to be independent of the increase in inhibitor concentration. The inhibitor was determined to be mixed type in 0.5 M H_2SO_4 and anodic type in 1 M H_2SO_4. Thermodynamic calculations showed the inhibition mechanism to be physiochemical. Adsorption of rosemary oil onto the steel surface fitted into the Langmuir model, thus proving that the molecular interaction is fixed. The surface topography remained unchanged in the presence of rosemay oil from Optical microscopy micrograhs.

REFERENCES

[1] EE Oguzie. *Corros. Sci.*, **2008**, 50(11), 2993-2998
[2] H Bentrah; Y Rahali; A Chala. *Corros. Sci.* **2014**, 82, 426-431
[3] A Ostovari; SM Hoseinieh; M Peikari; SR Shadizadeh; SJ Hashemi. *Corros. Sci*., **2009**, 51, 1935-1949
[4] VV Torres; RS Amado; C Faia de Sá; T.L. Fernandez; CADS Riehl; AG Torres; ED'Elia. *Corros. Sci.*, **2011**, 53, 2385-2392
[5] S Banerjee; V Srivastava; MM Singh. *Corros. Sci*., **2012**, 59, 35 -41
[6] MM Osman; MN Shalaby. *Mater. Chem. Phys*., **2003**, 77, 261-269
[7] PC Okafor; X Liu; YG Zheng. *Corros. Sci*., **2009**, 51, 761-768
[8] S Nešić; W Sun. Corrosion in acid gas solutions, JAR. Tony (Ed.), Shreir's Corrosion, Elsevier, Oxford, **2010**; 1270
[9] V Garcia-Arriaga; J Alvarez-Ramirez; M Amaya; E Sosa. *Corros. Sci.*, **2010**, 52, 2268-2279
[10] EE Ebenso. *Bull Electrochem* 2003, 19, 209-216
[11] DQ Zhang; LX Gao; GD Zhou. *J. Appl. Electrochem.*, **2003**, 33, 361-366.
[12] IL Rozenfeld. Corrosion Inhibitors, McGraw-Hill, New York, **1981**; 182
[13] M Abdallah; H Basim; IZ Asghar; AS Fouda. *Int. J. Electrochem. Sci.*, **2012**, 7(1), 282-304
[14] M Abdel-Aal; MS Morad. *Br. Corros. J*., **2001**, 36, 250.
[15] M Abdallah: MM El-Naggar. *Materials Chem. and Phys.*, **2001**, 71, 291-298.
[16] M Bonklah; A Quassini; B Hammouti; A El-Idrissi. *Appl. Surf. Sci*., **2006**, 252, 2178-2185
[17] M Abdallah; HE Megahed; MS Motae. *Mater. Chem. and Phys.*, **2009**, 118, 111-117
[18] SA. Abd El-Maksoud; AS Fouda. *Mater. Chem. and Phys.*, **2005**, 95, 84-88
[19] SS Abd El-Rehim; MAM Ibrahim; KF Khaled. *J. Appl Electrochem.*, **1999**, 29, 593-599.
[20] M Abdallah; ME Moustafa. *Annali di Chimica (Rome)*., **2004**, 94(7-8), 601-611.
[21] A Popora; E Sokolova; S Raicheva; M Christov. *Corros. Sci.*, **2003**, 45, 33-58
[22] M Sobhi; M Abdallah; KS Khairou. *Monatshefte fur Chemie.*, **2012**, 143, 1379-1387.
[23] M Abdallah; I Zaafarany; KS Khairou; M Sobhi. *Int. J. Electrochem. Soc.*, **2012**, 7(2), 1564-1579
[24] RS Felicia; S Santhanalakshmi; SJ Wilson; AA John; R Susai. *Bull. of Elect*., 2004, 20(12), 561-565.
[25] EB El-Anadouli. *Corros. Sci*., **1993**, 34(5), 779-784.
[26] P Agarwal; D Landolt. *Corros. Sci.*, **1998**, 40, 673-691.
[27] M Sahin; S Bilgiç; H Yılmaz. *App. Surf. Sci.*, 2002, 195(104), 1-7.
[28] RFV Villamil; P Corio; JC Rubin; SMI Agostinho. *J. of Elect. Chem.* 1999, 472, 112-119.